

# Growth of mutual information in a quenched one-dimensional open quantum many body system

Somnath Maity, Souvik Bandyopadhyay, Sourav Bhattacharjee and Amit Dutta  
*Department of Physics, Indian Institute of Technology Kanpur, Kanpur 208016, India*

We study the temporal evolution of the mutual information (MI) in a one-dimensional transverse Ising chain, coupled to a local fermionic Markovian bath, subsequent to a global quench of the transverse field. In the unitary case, the MI (or equivalently the bipartite entanglement entropy) saturates to a steady state value (obeying a volume law) following a ballistic growth. On the contrary, we establish that in the dissipative case the MI is exponentially damped both during the initial ballistic growth as well as in the approach to the steady state. The functional form proposed to describe the time dependence of the MI, which matches perfectly with the numerical results, suggests that information propagates solely through entangled pairs of quasi-particles having a finite life time; this quasi-particle picture is further corroborated by the analysis of two-point correlations. Remarkably, in spite of the finite life time of the quasi-particles, a finite steady state value of the MI survives which is an artefact of non-vanishing two points correlations. Further, the finite life time renders a finite length scale in this steady state correlations resulting in a sub-volume law of the MI.

*Introduction*– The entanglement entropy (EE) is an important measure of quantum correlations in a quantum many body system that also exhibits universal properties in the vicinity of a quantum phase transitions[1–4]. For a closed quantum system, the bipartite EE is calculated through the Von-Neumann entropy of the reduced density matrix  $\rho_\ell$  for a sub-system of size  $\ell$ ;

$$S(\ell) = -\text{Tr}[\rho_\ell \ln \rho_\ell], \quad (1)$$

where  $\rho_\ell = \text{Tr}_{L-\ell}[\rho_L]$  and  $\rho_L$  is the density matrix of the composite system of size  $L$ . If we consider the ground state of a short-range one-dimensional Hamiltonian, the EE follows an area law with a logarithmic correction of the form  $\sim \ln \ell$  when the composite system is at its quantum critical point[5, 6].

Recently, there has been a great interest in studying the temporal evolution of the EE of a closed quantum many body system following a quantum quench in which a parameter of the Hamiltonian is instantaneously changed [7]. The out-of-equilibrium dynamics of the system results in propagation of quantum correlations over the whole system thus leading to a growth of non-trivial bipartite entanglement even if the initial state is completely unentangled. It has been established [8] that following a global quench of a one-dimensional free fermionic Hamiltonian,  $S(\ell, t)$  exhibits a ballistic growth,  $S(\ell, t) \sim t$ , up to a time  $t^* = \ell/2v_{\max}$ , where  $v_{\max}$  is the maximum group velocity of information propagation. For  $t > t^*$ ,  $S(\ell, t)$  saturates to a constant value proportional to  $\ell$ , and hence the EE satisfies a volume law in the steady state.

The ballistic growth and the volume law scaling have also been verified in other models [9] and have been experimentally simulated [10]. For disordered spin chains [11–13], many body localized (MBL) phases [14–17] and also for local quenches [18–23] a characteristic logarithmic growth of the EE has been observed.

The out-of-equilibrium dynamics of the EE have also been studied both in periodically [24–27] and aperiodically [28, 29] driven free fermionic systems.

The purpose of this work is to investigate an area unexplored till date, namely how the dynamical generation of the bipartite entanglement following a global quench is influenced when the composite system is coupled to a weak *dissipative* environment. Notably, a dissipative coupling to an environment is likely to result in generation of entanglement between the composite system and the bath so that the former is no longer in a pure state. Consequently, the bipartite EE as defined in Eq. (1) is no longer significant as a measure of entanglement [4]. Particularly, we note that a correct measure of entanglement should be equivalent to the mutual information (MI), as is in the case of a pure composite state [4].

It is important to realise that a brute-force calculation of the von Neumann entropy for a sub-system using Eq. (1) will also have contribution from  $S(\rho_L)$ . For our analysis, we model the dynamical evolution of our system within a Lindbladian framework under the Born-Markov and secular approximations [30–32]. Interestingly, as we shall demonstrate below, the contribution from  $S(\rho_L)$  can be filtered out for some *particular choice of Lindblad operators*, to define a new quantity that has a direct correspondence with the MI.

In the unitary situation [8], the post-quench growth of the EE (or equivalently the MI) has been phenomenologically explained within a quasi-particle picture with quasi-particles having infinite life time. In the dissipative case, we find that the ballistic growth in MI is exponentially suppressed suggesting a finite life-time of the quasi-particles generated after the quench. Nevertheless, a finite MI persists in the asymptotic steady state which interestingly follows a sub-volume law.

*Mutual information*– The MI is defined as [4]:

$$I(\ell : L - \ell) = S(\rho_\ell) + S(\rho_{L-\ell}) - S(\rho_L), \quad (2)$$

where  $S(\rho_\ell)$ ,  $S(\rho_{L-\ell})$  and  $S(\rho_L)$  are the von-Neumann entropies of the sub-system, rest of the system and the composite system, respectively. For a *closed* system,  $S(\rho_L) = 0$  and  $S(\rho_\ell) = S(\rho_{L-\ell})$ ; consequently, the MI is equivalent to the bipartite EE in the unitary case. However, for a mixed  $\rho_L$ ,  $S(\rho_\ell) \neq S(\rho_{L-\ell}) \neq I(\ell : L - \ell)/2$ .

By splitting the quantity  $S(\rho_L)$  into two parts, we can rewrite Eq. (2) as

$$I(\ell : L - \ell) = S'(\ell) + S'(L - \ell) \quad (3)$$

where

$$S'(\ell) = S(\rho_\ell) - \frac{\ell}{L} S(\rho_L), \quad (4)$$

$$S'(L - \ell) = S(\rho_{L-\ell}) - \frac{L - \ell}{L} S(\rho_L). \quad (5)$$

Interestingly, in our case,  $S'(\ell) = S'(L - \ell) = I(\ell : L - \ell)/2$  (as verified in the supplementary material [33]). In hindsight, this factorization of  $S(\rho_L)$  is meaningful because the Lindbladian operators we consider here act independently on each site with uniform coupling strengths.

*Model and the bath*– In this work, we consider a transverse field Ising chain (TFIC) globally coupled to a Markovian bath [30, 32] (see [33] for detail). The chain is prepared in the unentangled ground state of the Hamiltonian with a large negative value of the transverse field ( $h$ ) which is instantaneously quenched to the final critical value  $h_f = 1$ .

The TFIC is described by the Hamiltonian

$$H = - \sum_{n=1}^L \sigma_n^x \sigma_{n+1}^x - h \sum_{n=1}^L \sigma_n^z, \quad (6)$$

where  $\sigma_n$ 's are the Pauli spin matrices for the  $n^{\text{th}}$  site. This can be mapped to a system of spinless fermionic model through a Jordan-Wigner (JW) transformation[34–38]; following a Fourier transformation to the quasi-momentum basis, the Hamiltonian decouples to the form:  $H = \sum_{k>0} H_k$ . In the basis spanned by the states  $\{|\phi_1^k\rangle = |0\rangle, |\phi_2^k\rangle = c_k^\dagger |0\rangle, |\phi_3^k\rangle = c_{-k}^\dagger |0\rangle, |\phi_4^k\rangle = c_k^\dagger c_{-k}^\dagger |0\rangle\}$ , where  $c_k^\dagger$  is the fermionic creation operator for the mode  $k$  and  $|0\rangle$  refers to the fermionic vacuum,  $H_k$  assumes a  $4 \times 4$  form (see [33]).

We choose a specific Markovian bath where system-bath interaction characterised by a set of JW *local* Lindblad operators  $\mathcal{L}_n = c_n$  (fermionic annihilation operator at site  $n$ ) [39–41]. The efficacy of such a choice of Lindbladian operator is that in the case of homogenous coupling strengths ( $\kappa_n = \kappa, \forall n$ ), the Lindblad master equation (with  $\hbar = 1$ ) decouples in the momentum modes as

$$\frac{d\rho_k(t)}{dt} = -i[H_k, \rho_k(t)] + \mathcal{D}_k[\rho_k(t)], \quad (7)$$

with

$$\begin{aligned} \mathcal{D}_k[\rho_k(t)] = & \kappa \left( c_k \rho_k(t) c_k^\dagger - \frac{1}{2} \left\{ c_k^\dagger c_k, \rho_k(t) \right\} \right. \\ & \left. + c_{-k} \rho_k(t) c_{-k}^\dagger - \frac{1}{2} \left\{ c_{-k}^\dagger c_{-k}, \rho_k(t) \right\} \right) \end{aligned} \quad (8)$$

evidently retaining the form  $\rho(t) = \otimes_{k>0} \rho_k(t)$  at all  $t$ . Unlike the unitary case, the dissipator breaks the parity conservation of fermion number in the dynamics [34] and one needs to retain both the parity sectors leading to a  $4 \times 4$  form of the density matrix in the basis  $\{|\phi_j^k\rangle\}$ :

$$\rho_k(t) = \sum_{i,j=1}^4 \rho_{ij}^k |\phi_i^k\rangle \langle \phi_j^k|. \quad (9)$$

*Numerical results*– The system is initially prepared in the unentangled ground state of the Hamiltonian  $H_k(h)$  with  $h \rightarrow -\infty$ , such that  $\rho_k(0) = |\phi_1^k\rangle \langle \phi_1^k|, \forall k$ . At  $t = 0+$ , the field  $h$  is suddenly changed to the critical value  $h_f = 1$  and the system evolves with the final Hamiltonian  $H(h_f)$  following Eq. (7). Numerically evaluating  $\rho_k(t)$ , we arrive at the two point correlations of fermions;

$$C_{mn}(t) = \text{Tr}[\rho(t), c_m^\dagger c_n], \quad F_{mn}(t) = \text{Tr}[\rho(t), c_m^\dagger c_n^\dagger] \quad (10)$$

where  $m, n = 1, 2, \dots, \ell$ . Finally, diagonalizing the  $2\ell \times 2\ell$  correlation matrix

$$\mathbb{C}_\ell = \begin{pmatrix} I - C & F \\ F^\dagger & C \end{pmatrix} \quad (11)$$

for the sub-system of size  $\ell$ , one can calculate  $S(\rho_\ell, t)$  and hence the MI ( $S'(\ell, t)$ ) for a free fermionic model [44] (see [33]).

*Unitary situation*: For  $\kappa = 0$  [8], the temporal evolution of the MI is reproduced in Fig. 1(a). Indeed, the MI shows a ballistic growth up to a time  $t^* = \ell/2$  and subsequently saturates to a constant value which is proportional to  $\ell$ . We note that in the limit  $L \rightarrow \infty$ ,  $\ell \rightarrow \infty$  with  $\ell \ll L$ , the MI is expected to have a ballistic growth in time indefinitely. On the contrary, for any finite  $\ell$ , the MI follows the  $\ell \rightarrow \infty$  line only up to the time  $t = t^* = \ell/2$ . This behaviour of the MI has been explained by a semiclassical description in terms of entangled pair of quasi-particles with equal and opposite group velocities  $v$  and  $v_{max} = 1$ , so that correlations spread following a light-cone behavior[45]. Further, the steady state behaviour of the MI is an artefact of the infinite life time of the quasi-particles.

*Dissipative situation*: We now proceed to the case  $\kappa \neq 0$ ; the temporal variation of  $S'(\ell, t)$ , obtained from Eq. (4) using  $\rho_k(t)$ , is presented in Fig. 1(b) for different sub-system sizes  $\ell$ . Critically inspecting the results, we conclude that the temporal evolution of  $S'(\ell, t)$  is significantly different when compared to that of the MI with  $\kappa = 0$ . For a given  $\ell$ , we observe a monotonic non-linear growth of the entanglement after which it eventually decays to the steady state value. The difference with the

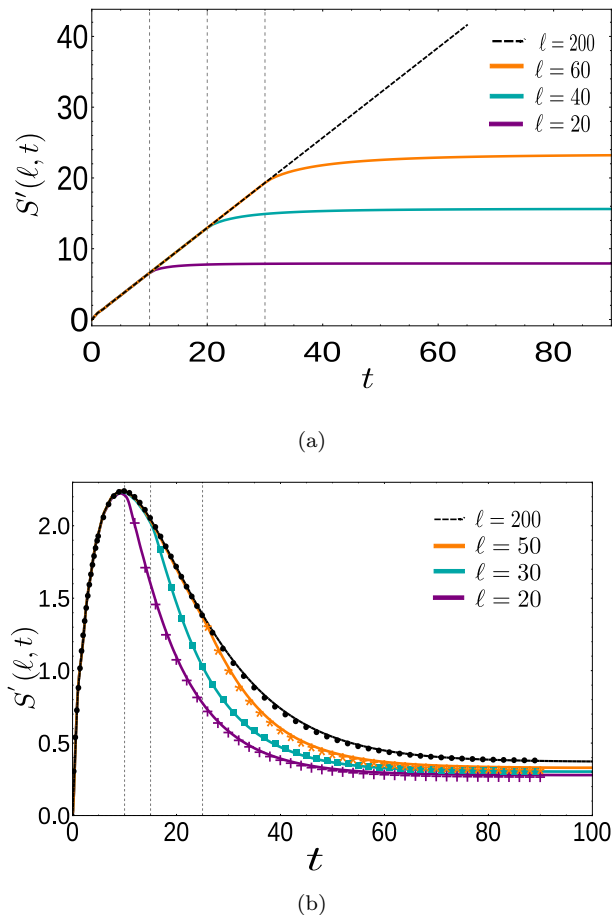


FIG. 1. (Color online) The time evolution of  $S'(\ell, t)$  for (a)  $\kappa = 0$  and (b)  $\kappa = 0.05$  with different sub-system size  $\ell$ . The black dashed line is for a large  $\ell = 200$  indicates the results in the limit  $\ell \rightarrow \infty$  (with  $\ell \ll L$ ). In (b), the markers denote the fits using the fitting functions defined in Eq. (12) for  $t < \ell/2$  and Eq. (13) for  $t > \ell/2$  as discussed in the text. Here, in both the case (a) and (b), the total system size  $L = 500$ .

$\kappa = 0$  situation is even more prominent in the limit  $L \rightarrow \infty$ ,  $\ell \rightarrow \infty$  with  $\ell \ll L$ , where, unlike the indefinite ballistic growth of MI expected in the former case,  $S'(\ell, t)$  is found to decay to a finite ( $\ell$  independent) steady value following the initial growth. However, similar to the case  $\kappa = 0$ , the deviation of  $S'(\ell, t)$  from  $S'(\ell \rightarrow \infty, t)$  again occurs at the same instant  $t = \ell/2$ ; this is because the unrenormalised Hamiltonian has been used in the unitary part of the master equation Eq. (7).

We propose the the following functional form of  $S'(\ell, t)$  in the limit  $\ell \rightarrow \infty$ :

$$S'(\ell \rightarrow \infty, t) \sim \mathcal{A} \left( 1 - e^{-c(\kappa)t} \right) + \mathcal{B} t e^{-d(\kappa)t}, \quad (12)$$

with  $c(\kappa) \gg d(\kappa)$  and the parameter  $\mathcal{B}$  is a non-universal constant depending on the group velocity of quasi-particles. Eq. (12) gives a perfect fitting with the numerically obtained results as depicted in Fig. 1(b). The functional form can be interpreted in the follow-

ing way: in early time limit,  $S'(\ell \rightarrow \infty, t) \sim \mathcal{B} t e^{-d(\kappa)t}$ , which essentially means that the linear growth in the MI observed in the  $\kappa = 0$  situation is now exponentially suppressed. This suppression can be attributed to the finite life-time of the quasi-particles in the case of finite dissipation. However, a finite MI survives in the asymptotic steady state,  $S'(\ell \rightarrow \infty, t \rightarrow \infty) = \mathcal{A}$ . We argue below that, most surprisingly, this remanent MI is indeed sustained by continuously generated quasi-particles due to perpetual coupling with bath, a fact that is manifested in two-point correlations.

Following the insight obtained from the  $\kappa = 0$  situation, it is natural to expect that for a finite  $\ell$ , the early time growth of the MI ( $\sim t e^{-d(\kappa)t}$ ) will continue as long as the quasi-particles originating from the centre of the sub-system do not cross the sub-system boundary, following which the MI will only decay exponentially, i.e.  $\sim e^{-d(\kappa)t}$ . This is what we indeed observe in Fig. 1(b). We therefore arrive at a modified functional form for  $t > \ell/2$ ,

$$S'(\ell, t) \sim \mathcal{P}(\ell, \kappa) + \frac{\mathcal{B}\ell}{2} e^{-d(\kappa)t}, \quad (13)$$

which again fits perfectly with the numerical results (Fig. 1(b)). The steady state value  $\mathcal{P}(\ell, \kappa)$  approaches  $\mathcal{A}$  in the limit  $\ell \rightarrow \infty$ ; very interestingly this steady value neither satisfies a perfect volume law nor an area law, rather is found to follow a sub-volume law (as presented in Fig. [S2] of [33]). This sub-volume behavior is a consequence of a finite length scale appearing in the steady state two point correlations (TPCs) of fermions, as we discuss below.

*Two point correlations*– For a free fermionic system, the time evolved density matrix (and hence any observable like the EE and the MI) is entirely characterised by the TPCs given in Eq. (10). A proper analysis of the influence of the bath on the same may therefore be instrumental in understanding the behavior of the  $S'(\ell, t)$  presented above.

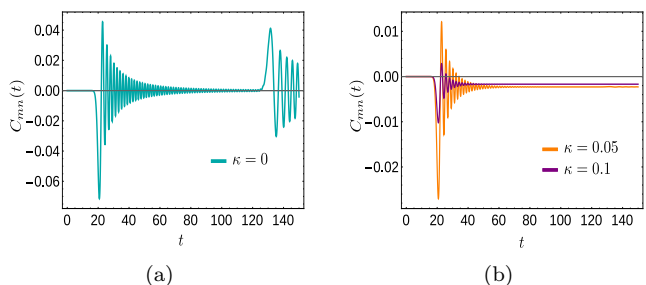


FIG. 2. (Color online) This figure shows the time evolution of the two point correlation  $C_{mn}(t)$  for (a)  $\kappa = 0$  and (b)  $\kappa = 0.05, 0.1$  under the quenching protocol ( $h = -\infty$  to  $h = 1$ ). We have considered two fixed sites  $m$  and  $n$  with  $|m - n| = 40$ , and  $L = 300$ .

For a translationally invariant system with periodic

boundary conditions, the single particle TPC,  $C_{mn}(t)$ , between sites  $m$  and  $n$  depends on the distance between the two sites (either  $|m - n|$  or  $L - |m - n|$ ). In Fig. 2, we plot the temporal evolution of  $C_{mn}(t)$  for different values of  $\kappa$ . For the unitary case ( $\kappa = 0$ ), a finite correlation begins to develop only after a time  $t = \min\{|(m - n)/2|, |(L - m + n)/2|\}$ . The existence of a finite correlation between the two sites ‘ $m$ ’ and ‘ $n$ ’ at a particular instant of time can now be attributed to the arrival of one quasi-particle of an entangled pair at site  $m$  and the other at site  $n$  at the same time. This evidently ensures that *only* the quasi-particles originating at the middle of either of the two segments between the two points can contribute to the two point correlations. Since the minimum time taken by these quasi-particles to arrive at the two sites is given by  $t^* = \min\{|(m - n)/2|, |(L - m + n)/2|\}$ , no finite correlation is observed for  $t < t^*$ . The successive peaks occur due to the slower moving quasi-particles ( $v(k) < v_{max}$ ). The slower moving quasi-particles are less abundant than the faster moving ones, as evident from the progressively decreasing amplitude of the subsequent peaks. A revival of correlation can occur due to the arrival of the quasi-particles from the middle of the longer segment connecting the two points as observed in Fig. 2(a). We note that in the thermodynamic limit  $L \rightarrow \infty$  and for a finite  $|m - n| \ll L$ , this revival can not occur.

Importantly, even for the case  $\kappa \neq 0$ , no finite correlation is observed for  $t < t^*$ . As already mentioned, we note that the maximum velocity of the quasi-particles is same as in the unitary case. The amplitude of the correlations are also smaller as compared to the  $\kappa = 0$  case with the amplitude of the revivals significantly diminished. This supports the fact that the quasi-particles originating at  $t = 0$  now has a finite life time. Further, the two point correlation saturates to a finite non-zero value unlike the  $\kappa = 0$  case as shown in the Fig. 2(b). This is manifested also in the non-zero steady state value of the  $S'(\ell, \infty)$  as analysed in [33].

Finally, the steady state TPC when plotted as a function of the (shorter) intermediate distance  $|m - n|$ , (as shown in Fig. 3 for different values of  $\kappa$ ) shows an exponential decay of the form,

$$C_{mn}(\infty) \sim \exp\left\{-\frac{\kappa(m - n)}{2}\right\}. \quad (14)$$

This implies that when the  $|n - m|$  exceeds  $2/\kappa$ , the quasi-particles generate negligible correlations, thereby pointing to a finite length scale,  $\xi_\kappa = 2/\kappa$ , of the steady state TPCs.

The above analysis of the TPCs have following bearing on the behaviour of  $S'(\ell, t)$  discussed earlier. Since the group velocity of the entangled pair of quasi-particles remain unaltered for  $\kappa \neq 0$ , we observe that the deviation in  $S'(\ell, t)$  from the  $\ell \rightarrow \infty$  curve occurs at  $t^* = \ell/2$  as for  $\kappa = 0$ . The remanent TPC in the steady state is reflected

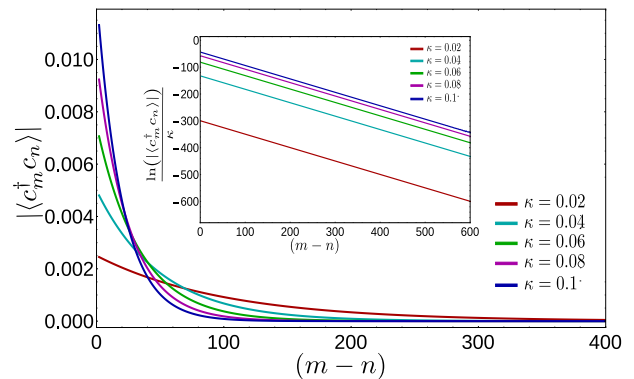


FIG. 3. (Color online) The variation of  $C_{mn}(\infty)$  in the steady state with the distance  $(m - n)$  for different values of  $\kappa$ . In the inset, we have plotted the quantity  $\ln(|C_{mn}(\infty)|)$  scaled by  $\kappa$  with respect to  $(m - n)$ . This shows a linear behaviour for all  $\kappa$  having a slope equal to 0.5, suggesting an exponential decay (Eq. (14)) of the steady state TPCs.

in the non-zero steady state value of  $S'(\ell, t)$ . This steady state MI, however, results from the collective contribution of remanent TPCs between sites that are located within a finite distance ( $\sim \xi_\kappa$ ) from either end of the sub-system. The remanent TPCs can be attributed to a *continuous* generation of quasi-particles due to perpetual coupling with bath as discussed in [33]. We note that this is significantly different from the  $\kappa = 0$  case where the finite MI at large time is maintained collectively by TPCs between all sites of the system.

Further, the finite life time of quasi-particles results in an exponential suppression of the MI at all instants of time. Finally, a *no-quench* analysis of the TPC (elaborated in [33]) reveals that the coupling to the bath also acts as a quench that induces correlations solely propagated by quasi-particles with finite lifetime.

In summary, we study the influence of a weak dissipative coupling on the generation and growth of the MI in a quenched one-dimensional integrable model. As in the unitary ( $\kappa = 0$ ) case, the MI acquires a finite steady value at long times; in this case however, the steady value is determined by both the post-quench Hamiltonian as well as the coupling strength with the bath and does not follow a volume law. Further, the ballistic growth due to the quench induced propagating correlations is exponentially damped due to the bath induced dissipation.

Souvik Bandyopadhyay acknowledges PMRF fellowship, MHRD, India and Sourav Bhattacharjee acknowledges CSIR, India for financial support.

- 
- [1] L. Amico, R. Fazio, A. Osterloh, and V. Vedral, *Rev.Mod.Phys.*, **80**, 517 (2008).  
 [2] J. I. Latorre, A. Riera, *J. Phys. A: Math. Theor.* **42** (2009)

- 504002.
- [3] J. Eisert, M. Cramer, and M. B. Plenio, *Rev. Mod. Phys.* **82**, 277 (2010).
- [4] M. A. Nielsen and I. L. Chuang, *Quantum Computation and Information*, Cambridge University Press, Cambridge (2010).
- [5] G. Vidal, J. I. Latorre, E. Rico, and A. Kitaev, *Phys. Rev. Lett.* **90**, 227902 (2003).
- [6] P. Calabrese and J. Cardy, *J. Stat. Mech.* (2004) P06002.
- [7] A. Polkovnikov, K. Sengupta, A. Silva, and M. Vengalattore *Rev. Mod. Phys.* **83**, 863 (2011).
- [8] P. Calabrese, and J. Cardy, *J. Stat. Mech.* (2005) P04010.
- [9] M. Fagotti, and P. Calabrese, *Phys. Rev. A* **78**, 010306 (R) (2008).
- [10] I. Pitsios, L. Banchi, A. S. Rab, M. Bentivegna, D. Caprara, A. Crespi, N. Spagnolo, S. Bose, P. Mataloni, R. Osellame, and F. Sciarrino, *Nat. Comm.* **8**, 1569 (2017).
- [11] G. D. Chiara, S. Montangero, P. Calabrese, and R. Fazio, *J. Stat. Mech.* (2006) P03001.
- [12] C. K. Burrell and T. J. Osborne, *Phys. Rev. Lett.* **99**, 167201 (2007).
- [13] F. Igli, Z. Szatmari, and Y. Lin, *Phys. Rev. B* **85**, 094417 (2012).
- [14] M. Znidaric, T. Prosen, and P. Prelovsek, *Phys. Rev. B* **77**, 064426 (2008).
- [15] J. H. Bardarson, F. Pollmann, and J. E. Moore, *Phys. Rev. Lett.* **109**, 017202 (2012).
- [16] R. Vosk and E. Altman, *Phys. Rev. Lett.* **112**, 217204 (2014).
- [17] P. Ponte, Z. Papi, F. Huveneers, and D. A. Abanin, *Phys. Rev. Lett.* **114**, 140401 (2015).
- [18] V. Eisler, and I. Peschel, *J. Stat. Mech.* (2007) P06005.
- [19] P. Calabrese, and J. Cardy, *J. Stat. Mech.* (2007) P10004.
- [20] V. Eisler, D. Karevski, T. Platini, and I. Peschel, *J. Stat. Mech.* (2008) P01023.
- [21] Jean-Marie Stephan, Jerome Dubail, *J. Stat. Mech.* (2011) P08019.
- [22] U. Divakaran, F. Igloi and H. Ruger, *J. Stat. Mech.* **11**, 10027 (2011).
- [23] A. Rajak, and U. Divakaran *J. Stat. Mech.* (2016) 043107.
- [24] V. Eisler and I. Peschel, *Ann. Phys. (Berlin)* **17**, 410 (2008).
- [25] A. Sen, S. Nandy, and K. Sengupta, *Phys. Rev. B* **94**, 214301 (2016).
- [26] A. Russomanno, G. E. Santoro and R. Fazio, *J. Stat. Mech.: Theory Exp.* (2016) 073101.
- [27] T. J. G. Apollaro, G. M. Palma, and J. Marino, *Phys. Rev. B* **94**, 134304 (2016).
- [28] S. Maity, U. Bhattacharya, and A. Dutta, *Phys. Rev. B* **98**, 064305 (2018).
- [29] S. Nandy, A. Sen, and D. Sen, *Phys. Rev. B* **98** 245144 (2018).
- [30] G. Lindblad, *Commun. Math. Phys.* **48**, 199 (1976).
- [31] C. W. Gardiner and P. Zoller, *Quantum Noise* (Springer, Heidelberg, 2000).
- [32] H. P. Breuer and F. Petruccione, *Theory of open quantum systems*, Oxford University Press, Oxford (2002).
- [33] See Supplemental Material (SM) for details of the model and bath, solution of  $\rho_k(t)$ , calculation of TPCs and the steady state behaviour of the MI.
- [34] E. Lieb, T. Schultz, and D. Mattis, *Ann. Phys.* **16**, 407 (1961).
- [35] J. B. Kogut, *Rev. Mod. Phys.* **51**, 659 (1979).
- [36] S. Sachdev, *Quantum Phase Transition*, Cambridge University Press, Cambridge (2011).
- [37] S. Suzuki, J. Inoue, and B. K. Chakrabarti, *Quantum Ising Phases and Transitions in Transverse Ising Models*, Lecture Notes in Physics 862 (Springer, 2013).
- [38] A. Dutta, G. Aeppli, B. K. Chakrabarti, U. Divakaran, T. F. Rosenbaum, D. Sen, *Quantum Phase Transitions in Transverse Field Spin Models*, Cambridge University Press, Cambridge (2015).
- [39] A. Carmele, M. Heyl, C. Kraus, M. Dalmonte, *Phys. Rev. B* **92**, 195107 (2015).
- [40] M. Keck, S. Montangero, G. E. Santoro, R. Fazio, D. Rossini, *New J. Phys.* **19** 113029 (2017).
- [41] S. Bandyopadhyay, S. Laha, U. Bhattacharya and A. Dutta, *Sci. Rep.* **8**, 11921 (2018).
- [42] L. Cincio, J. Dziarmaga, M. M. Rams, and W. H. Zurek, *Phys. Rev. A* **75**, 052321 (2007).
- [43] E. Canovi, E. Ercolessi, P. Naldesi, L. Taddia, and D. Vodola, *Phys. Rev. B* **89**, 104303 (2014).
- [44] I. Peschel, *J. Phys. A: Math. Gen.* **36**, L205-L208 (2003).
- [45] E.H. Lieb and D.W. Robinson, *Commun. Math. Phys.* **28**, 251 (1972).

# Supplemental Material on “Growth of mutual information in a critically quenched one-dimensional open quantum many body system”

## MODEL AND THE BATH

In this work, the subsequent dissipative dynamics of the transverse field Ising chain (TFIC) following a quench of the transverse field (from  $h = -\infty$  and  $h = 1$ ) is assumed to be described by a Lindblad master equation of the form[S1-3],

$$\frac{d\rho(t)}{dt} = -i[H, \rho(t)] + \mathcal{D}[\rho(t)]; \quad (\text{S1})$$

we have set  $\hbar = 1$  throughout. The first term on the right hand side describes the unitary time evolution evolution of the system's density matrix  $\rho(t)$  while the dissipator  $\mathcal{D}[\rho(t)]$  encapsulates the dissipative dynamics and assumes a form:

$$\mathcal{D}[\rho(t)] = \sum_n \kappa_n \left( \mathcal{L}_n \rho(t) \mathcal{L}_n^\dagger - \frac{1}{2} \{ \mathcal{L}_n^\dagger \mathcal{L}_n, \rho(t) \} \right), \quad (\text{S2})$$

where  $\mathcal{L}_n$  are the Lindblad operators with  $\kappa_n (\geq 0)$ 's being the corresponding dissipation strengths.

The transverse field Ising chain is described by the Hamiltonian

$$H = - \sum_{n=1}^L \sigma_n^x \sigma_{n+1}^x - h \sum_{n=1}^L \sigma_n^z, \quad (\text{S3})$$

where  $\sigma_n$ 's are the Pauli spin matrices for the  $n^{\text{th}}$  site and  $h$  is the transverse magnetic field. Considering anti-periodic boundary condition, the Eq. S3 can be mapped to a system of spinless fermions model through a Jordan-Wigner (JW) transformation, to arrive at the following quadratic form:

$$H = - \sum_{n=1}^L \left( c_n^\dagger c_{n+1} + c_n^\dagger c_{n+1}^\dagger + \text{h.c.} \right) + 2h (c_n^\dagger c_n), \quad (\text{S4})$$

where  $c_n$  ( $c_n^\dagger$ ) are Fermionic annihilation (creation) operators residing on the  $n$ -th site. Further, in the quasi-momentum basis, the Hamiltonian decouples as  $H = \sum_{k>0} H_k$ , with  $k = [2\pi(n+1/2)]/L$  where  $n \in \{0, 1, 2 \dots (L-1)\}$ . In the basis spanned by the states  $\{|\phi_1^k\rangle = |0\rangle, |\phi_2^k\rangle = c_k^\dagger |0\rangle, |\phi_3^k\rangle = c_{-k}^\dagger |0\rangle, |\phi_4^k\rangle = c_k^\dagger c_{-k}^\dagger |0\rangle\}$ ,  $H_k$  assumes the form

$$H_k = \begin{pmatrix} h - \cos k & 0 & 0 & \sin k \\ 0 & 0 & 0 & 0 \\ 0 & 0 & 0 & 0 \\ \sin k & 0 & 0 & -h + \cos k \end{pmatrix}. \quad (\text{S5})$$

For a specific system-bath interaction, as used in this work, characterised by a set of *local* Lindblad operators  $\mathcal{L}_n = c_n$  [S4, 5], the Lindblad master equation given in Eq. (S1) decouples in the momentum modes as

$$\frac{d\rho_k(t)}{dt} = -i[H_k, \rho_k(t)] + \mathcal{D}_k[\rho_k(t)], \quad (\text{S6})$$

with

$$\mathcal{D}_k[\rho_k(t)] = \kappa \left( c_k \rho_k(t) c_k^\dagger - \frac{1}{2} \{ c_k^\dagger c_k, \rho_k(t) \} + c_{-k} \rho_k(t) c_{-k}^\dagger - \frac{1}{2} \{ c_{-k}^\dagger c_{-k}, \rho_k(t) \} \right). \quad (\text{S7})$$

In the next section, we will cast the Eq. (S6) into a set of coupled differential equations in a particular choice of basis and solve the them numerically to find out  $\rho_k(t)$  in the present scenario .

## GENERAL SOLUTION OF $\rho(t)$

In this section, we will briefly elaborate the calculation of the density matrix  $\rho_k(t)$  for each momenta mode using the Eq. (S6)[S5, 6]. Let us recall the basis which we considered here,

$$|\phi_1^k\rangle \equiv |0, 0\rangle, \quad (\text{S8})$$

$$|\phi_2^k\rangle \equiv c_k^\dagger |0, 0\rangle = |k, 0\rangle, \quad (\text{S9})$$

$$|\phi_3^k\rangle \equiv c_{-k}^\dagger |0, 0\rangle = |0, -k\rangle, \quad (\text{S10})$$

$$|\phi_4^k\rangle \equiv c_k^\dagger c_{-k}^\dagger |0, 0\rangle = |k, -k\rangle, \quad (\text{S11})$$

where  $|0, 0\rangle$  and  $|k, -k\rangle$  refer both the fermionic states for  $c_k$  and  $c_{-k}$  are occupied and unoccupied, respectively. In the above basis, we have the following matrix forms of  $c_k$ ,  $c_{-k}$  and  $H_k(h)$  for each  $k$  mode

$$c_k = \begin{pmatrix} 0 & 1 & 0 & 0 \\ 0 & 0 & 0 & 0 \\ 0 & 0 & 0 & -1 \\ 0 & 0 & 0 & 0 \end{pmatrix}, \quad c_{-k} = \begin{pmatrix} 0 & 0 & 1 & 0 \\ 0 & 0 & 0 & 1 \\ 0 & 0 & 0 & 0 \\ 0 & 0 & 0 & 0 \end{pmatrix}, \quad \text{and} \quad H_k(h) = \begin{pmatrix} h - \cos k & 0 & 0 & \sin k \\ 0 & 0 & 0 & 0 \\ 0 & 0 & 0 & 0 \\ \sin k & 0 & 0 & -h + \cos k \end{pmatrix}. \quad (\text{S12})$$

Using the above equations, the Lindblad equation (Eq. [10] in the main text) for each  $k$  mode contains sixteen coupled first order linear differential equations of which only ten are independent, those are

$$\begin{aligned} \dot{\rho}_{11}(t) &= -i\Delta(\rho_{14}^*(t) - \rho_{14}(t)) + \kappa(\rho_{22}(t) + \rho_{33}(t)), \\ \dot{\rho}_{12}(t) &= -i(\epsilon\rho_{12}(t) + \Delta\rho_{24}^*(t)) - \kappa\left(\frac{1}{2}\rho_{12}(t) - \rho_{34}(t)\right), \\ \dot{\rho}_{13}(t) &= -i(\epsilon\rho_{13}(t) + \Delta\rho_{34}^*(t)) - \kappa\left(\frac{1}{2}\rho_{13}(t) - \rho_{24}(t)\right), \\ \dot{\rho}_{14}(t) &= -i(2\epsilon\rho_{14}(t) + \Delta\rho_{11}(t) + \Delta\rho_{44}(t)) - \kappa\rho_{14}(t), \\ \dot{\rho}_{22}(t) &= -\kappa\rho_{22}(t) + \kappa\rho_{44}(t), \\ \dot{\rho}_{23}(t) &= -\kappa\rho_{23}(t), \\ \dot{\rho}_{24}(t) &= -i(\epsilon\rho_{24}(t) - \Delta\rho_{12}^*(t)) - \frac{3\kappa}{2}\rho_{24}(t), \\ \dot{\rho}_{33}(t) &= -\kappa\rho_{33}(t) + \kappa\rho_{44}(t), \\ \dot{\rho}_{34}(t) &= -i(\epsilon\rho_{34}(t) - \Delta\rho_{13}^*(t)) - \frac{3\kappa}{2}\rho_{34}(t), \\ \dot{\rho}_{44}(t) &= -i\Delta(\rho_{14}(t) - \rho_{14}^*(t)) - 2\kappa\rho_{44}(t). \end{aligned} \quad (\text{S13})$$

where  $\epsilon = h - \cos k$ ,  $\Delta = \sin k$  and  $\dot{\rho}_{ij} = d\rho_{ij}/dt$ . Solving the above equations we can obtain  $\rho_k(t)$ . It is evident from the above equations that if we consider the initial state prepared at  $h_i = -\infty$  i.e.,  $\rho_k(0) = |0, 0\rangle\langle 0, 0|$ , the density matrix  $\rho_k(t)$  has only five non-zero elements,  $\rho_{11}(t)$ ,  $\rho_{22}(t)$ ,  $\rho_{33}(t)$ ,  $\rho_{44}(t)$ , and  $\rho_{14}(t)$ . Thus, at any instant of time  $t$ , the density matrix for each  $k$  mode takes the following form

$$\rho_k(t) = \begin{pmatrix} \rho_{11}(t) & 0 & 0 & \rho_{14}(t) \\ 0 & \rho_{22}(t) & 0 & 0 \\ 0 & 0 & \rho_{33}(t) & 0 \\ \rho_{14}^*(t) & 0 & 0 & \rho_{44}(t) \end{pmatrix}. \quad (\text{S14})$$

Having the solutions of  $\rho_k(t)$ , we can proceed to calculate the fermionic two point correlations (TPCs) and eventually the mutual information (MI)  $S'(\ell, t)$ .

## CALCULATION OF FERMIONIC TWO POINT CORRELATIONS

We now present the calculation of fermionic two point correlation functions using the density matrix  $\rho_k(t)$ . Let us first write the Fourier transform of the JW fermion  $c_n$  for the momenta  $k > 0$

$$c_n = \frac{1}{\sqrt{L}} \sum_{k>0} (e^{-ikn} c_k + e^{ikn} c_{-k}). \quad (\text{S15})$$

Using the Eq. (S15), one can write the two point correlations (TPCs) in real space in terms of TPCs in the momentum space as

$$\begin{aligned}\langle c_m^\dagger c_n \rangle &= \frac{1}{L} \sum_{k_1, k_2 > 0} \left( e^{i(k_1 m - k_2 n)} \langle c_{k_1}^\dagger c_{k_2} \rangle + e^{i(k_1 m + k_2 n)} \langle c_{k_1}^\dagger c_{-k_2} \rangle + e^{-i(k_1 m + k_2 n)} \langle c_{-k_1}^\dagger c_{k_2} \rangle + e^{-i(k_1 m - k_2 n)} \langle c_{-k_1}^\dagger c_{-k_2} \rangle \right), \\ \langle c_m^\dagger c_n^\dagger \rangle &= \frac{1}{L} \sum_{k_1, k_2 > 0} \left( e^{i(k_1 m + k_2 n)} \langle c_{k_1}^\dagger c_{k_2}^\dagger \rangle + e^{i(k_1 m - k_2 n)} \langle c_{k_1}^\dagger c_{-k_2}^\dagger \rangle + e^{-i(k_1 m - k_2 n)} \langle c_{-k_1}^\dagger c_{k_2}^\dagger \rangle + e^{-i(k_1 m + k_2 n)} \langle c_{-k_1}^\dagger c_{-k_2}^\dagger \rangle \right),\end{aligned}\tag{S16}$$

where all the expectation values on the right hand side are taken over the momentum space density matrix  $\rho(t) = \otimes_{k>0} \rho_k(t)$  i.e. for a general operator  $\hat{O}$ ;

$$\langle \hat{O}(t) \rangle = \text{Tr} \left[ \rho(t) \hat{O} \right] = \sum_{k>0} \sum_{i,j=1}^4 \rho_{i,j}^k(t) \langle \phi_j^k | \hat{O} | \phi_i^k \rangle. \tag{S17}$$

Using the Eq. (S17) and Eqs. (S8)-(S11), one can calculate the following correlations in momentum space;

$$\langle c_{k_1}^\dagger c_{k_2} \rangle = \sum_{k>0} \sum_{i,j=1}^4 \rho_{i,j}^k \langle \phi_j^k | c_{k_1}^\dagger c_{k_2} | \phi_i^k \rangle = \sum_{k>0} (\rho_{22}^k + \rho_{44}^k) \delta_{k_1, k_2} \delta_{k_1, k}, \tag{S18}$$

$$\langle c_{-k_1}^\dagger c_{-k_2} \rangle = \sum_{k>0} (\rho_{33}^k + \rho_{44}^k) \delta_{k_1, k_2} \delta_{k_1, k}, \tag{S19}$$

$$\langle c_{k_1}^\dagger c_{-k_2} \rangle = \sum_{k>0} (\rho_{32}^k) \delta_{k_2, k} \delta_{k_1, k}, \tag{S20}$$

$$\langle c_{-k_1}^\dagger c_{k_2} \rangle = \sum_{k>0} (\rho_{23}^k) \delta_{k_2, k} \delta_{k_1, k}, \tag{S21}$$

and

$$\langle c_{k_1}^\dagger c_{k_2}^\dagger \rangle = 0, \tag{S22}$$

$$\langle c_{-k_1}^\dagger c_{-k_2}^\dagger \rangle = 0, \tag{S23}$$

$$\langle c_{k_1}^\dagger c_{-k_2}^\dagger \rangle = \sum_{k>0} (\rho_{14}^k) \delta_{k_2, k} \delta_{k_1, k}, \tag{S24}$$

$$\langle c_{-k_1}^\dagger c_{k_2}^\dagger \rangle = - \sum_{k>0} (\rho_{14}^k) \delta_{k_2, k} \delta_{k_1, k}. \tag{S25}$$

Note that in the last equation the negative sign comes from fermionic anti-commutation relations i.e. using the fact  $c_{-k}^\dagger c_k^\dagger |0, 0\rangle = -|k, -k\rangle$ . Finally, using the above correlation functions in Eqs. (S18)-(S25) and Eq. (S16), the elements in the correlation matrix  $\mathcal{C}$  for the sub system of size  $\ell$  can be found as

$$\begin{aligned}C_{mn}(t) &= \frac{1}{L} \sum_{k>0} (\rho_{22}^k + \rho_{44}^k) e^{ik(m-n)} + \rho_{32}^k e^{ik(m+n)} + \rho_{23}^k e^{-ik(m+n)} + (\rho_{33}^k + \rho_{44}^k) e^{-ik(m-n)} \\ &= \frac{2}{L} \sum_{k>0} \rho_{44}^k \cos(k(m-n)) + \frac{1}{L} \sum_{k>0} \left\{ \rho_{22}^k e^{ik(m-n)} + \rho_{33}^k e^{-ik(m-n)} \right\}\end{aligned}\tag{S26}$$

$$F_{mn}(t) = \frac{2}{L} \sum_{k>0} \rho_{14}^k \sin(k(m-n)) \tag{S27}$$

where  $m, n = 1, 2, 3, \dots, \ell$  and the time dependence comes from the time dependent matrix elements  $\rho_{ij}^k(t)$  of the density matrix  $\rho_k(t)$ . Note that in arriving at the final form of the Eq. (S26), we have used the fact that  $\rho_{23}^k(t) = \rho_{32}^k(t) = 0$  valid for the present choice of initial conditions (see Eq. (S14)). In the unitary case ( $\kappa = 0$ ),  $\rho_{22}^k(t)$  and  $\rho_{33}^k(t)$  vanish, rendering a simpler form of the  $C_{mn}(t)$ .

In our numerical scheme, by solving Eqs. (S13), we shall construct the density matrix given in the Eq. (S14) and hence evaluate Eq. (S26) and Eq. (S27). Having the values of TPCs  $C_{mn}(t)$  and  $F_{mn}(t)$ , we construct the correlation (or covariance) matrix  $\mathbb{C}_\ell$  (Eq. [12] in the main text) and proceed to calculate the von-Neumann entropy  $S(\rho_\ell)$  of the reduced density matrix  $\rho_\ell$  of a sub-system of size  $\ell$  as

$$S(\rho_\ell) = - \sum_{i=1}^{2\ell} \lambda_i \ln \lambda_i \tag{S28}$$

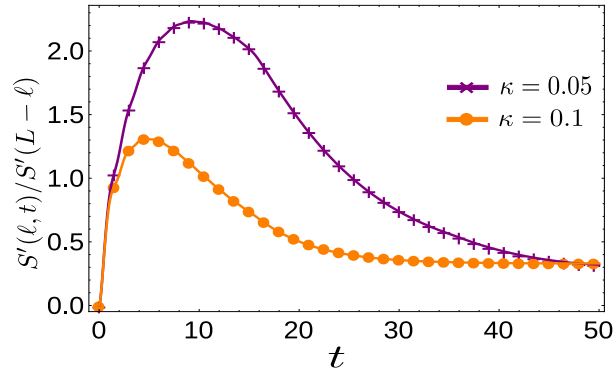


FIG. S1. (Color online) This figure shows that  $S'(\ell, t)$  (denoted by solid lines) is equal to  $S'(L-\ell, t)$  (denoted by markers) for all instants of time. We have chosen two values of the coupling strength  $\kappa = 0.05$  and  $0.1$ , the sub-system size  $\ell = 30$  and the composite system size  $L = 100$

where  $\lambda_i$  are the eigenvalues of the correlation matrix  $\mathbb{C}_\ell$  [S7].

### NUMERICAL VERIFICATION OF $S'(\ell, t) = S'(L-\ell, t)$ FOR ALL $t$

Let us recall, the definition of the mutual information (MI)

$$I(\ell : L-\ell) = S(\rho_\ell) + S(\rho_{L-\ell}) - S(\rho_L), \quad (\text{S29})$$

where  $S(\rho_\ell)$ ,  $S(\rho_{L-\ell})$  and  $S(\rho_L)$  are the von-Neumann entropy of the sub-system, rest of the system and the composite system, respectively. By splitting the quantity  $S(\rho_L)$  into two parts, we can rewrite the above equation in following way

$$I(\ell : L-\ell) = S'(\ell) + S'(L-\ell) \quad (\text{S30})$$

where

$$S'(\ell) = S(\rho_\ell) - \frac{\ell}{L}S(\rho_L), \quad \text{and} \quad S'(L-\ell) = S(\rho_{L-\ell}) - \frac{L-\ell}{L}S(\rho_L). \quad (\text{S31})$$

Interestingly, for the bath chosen in the present work, the two quantity  $S'(\ell)$  and  $S'(L-\ell)$  are exactly equal in all time as shown in the Fig. S1.

### STEADY STATE SOLUTION OF $\rho_k(t)$

In the presence of the dissipative environment, following a sudden quench the system reaches a steady state in the asymptotic limit of time  $t \rightarrow \infty$ . In the present scenario, analytical form of the steady state density matrix  $\rho_k(\infty)$  for each  $k$  mode can be exactly calculated by putting  $d\rho_k(t)/dt = 0$  in the Lindblad master equation (S6). The non-zero elements of the density matrix  $\rho_k(\infty)$  assume the following form:

$$\rho_{11}(\infty) = \frac{\Delta^2 + 4\epsilon^2 + \kappa^2}{4(\Delta^2 + \epsilon^2) + \kappa^2}, \quad (\text{S32})$$

$$\rho_{22}(\infty) = \rho_{33}(\infty) = \rho_{44}(\infty) = \frac{\Delta^2}{4(\Delta^2 + \epsilon^2) + \kappa^2}, \quad (\text{S33})$$

$$\rho_{14}(\infty) = \frac{\Delta(2\epsilon - i\kappa)}{4(\Delta^2 + \epsilon^2) + \kappa^2}, \quad (\text{S34})$$

where  $\epsilon = h_f - \cos k$  and  $\Delta = \sin k$ . These solutions enable us to calculate the steady state two point correlations  $C_{mn}(\infty)$ ,  $F_{mn}(\infty)$  and the steady state von Neumann entropy  $S(\ell, \infty)$  of a sub-system of size  $\ell$ . Further, the steady state MI  $S'(\ell, t)$ , calculated using Eq. (S31), is shown in the Fig. S2. Interestingly, the steady state MI neither shows a volume law or area law; rather it shows a sub-volume law as also mentioned in the main text.

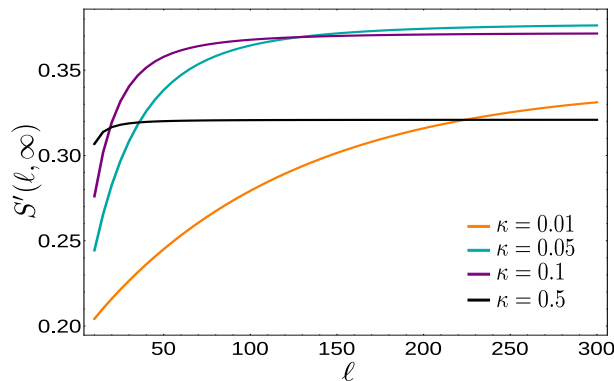


FIG. S2. (Color online) The variation of the steady state value of MI  $S'(\ell, t)$  (i.e.,  $\mathcal{P}(\ell, \kappa)$  in Eq. [14] of the main text ) with  $\ell$  for different values of  $\kappa$ . As  $\kappa$  increases from 0 to higher values,  $\mathcal{P}(\ell, \kappa)$  approaches from a volume law to an area law through an intermediate sub volume region. Here, we choose  $L = 1000$ .

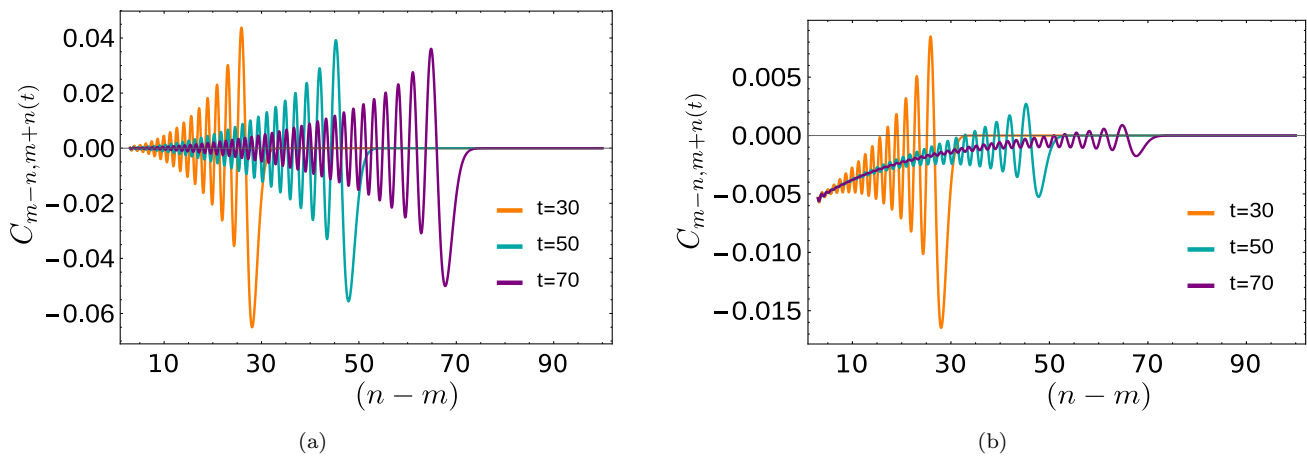


FIG. S3. (Color online). Here, we plot the two-point correlations  $C_{mn}(t)$  between pairwise points (labelled by  $n$ ) equidistant from the site  $m$  (chosen to be  $m = 50$ ) for different instants of time after the sudden quench of the transverse field for (a) the unitary case ( $\kappa = 0$ ) and (b) the dissipative case ( $\kappa \neq 0$ ).

### STEADY STATE MI FROM TWO-POINT CORRELATIONS

In this section, we study the dynamics of two-point correlations (TPCs)  $C_{mn}(t)$  (given in the Eq. (S26)) further to understand the origin of finite non-zero value of the steady state MI for the dissipative case. Here, we calculate the equal-time single particle TPCs between pairwise points equidistant from a fixed site (denoted by  $m$ );

$$C_{m-n, m+n}(t) = \langle c_{m-n}^\dagger(t) c_{m+n}(t) \rangle \quad (\text{S35})$$

by varying  $n (\geq 1)$ . In Fig. S3, we plot  $C_{m-n, m+n}(t)$  as a function of  $(n - m)$  for different instants of time. The two points  $m + n$  and  $m - n$  become correlated only when entangled pair of quasi-particles reach the two points simultaneously. This essentially implies that only the quasi-particles originating at the mid point  $m$  can contribute to  $C_{m-n, m+n}(t)$  at any time  $t > 0$ . Note that we have ignored possible contributions from the mid-point of the other segment ( $L - 2n$ ) due to the circular geometry of the chain; this is a valid approximation as  $L \gg 2n$ . Thus, it is clear that, at a given time  $t$ , only the points lying within distance  $m - n = v_g t = t$  can have finite pair-wise correlation with their corresponding counter parts in the segment  $m + n$ , as is clearly seen in Fig S3. As discussed in the main text, the subsequent peaks after the first peak, i.e. within the region  $|n - m| < t$ , is due to the presence of the slower moving quasi-particles. In the unitary case (see Fig. 3(a)), the resultant correlation profile evolves in a packet like fashion with its front end propagating with maximum group velocity ( $v_{max} = 1$ ) while the tail end elongates in time due to the velocity differences between quasi-particles. In the dissipative case, however, the correlation profile evolves with a non-vanishing tail even though its front end continue to propagate with velocity  $v_{max}$  but with a rapidly diminishing

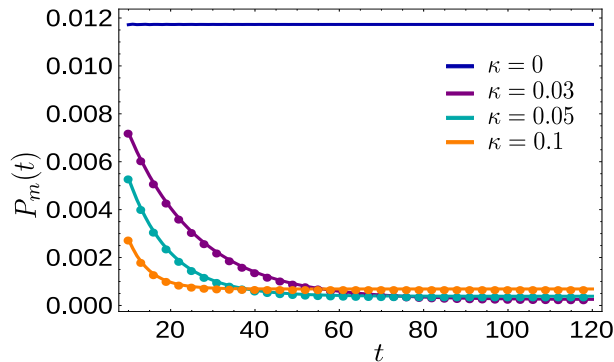


FIG. S4. (Color online) Here, we plot the quantity  $P_m(t)$  with time  $t$  for different values of  $\kappa$ . The markers on curves for  $\kappa \neq 0$  are obtained using the fitted function  $\alpha(\kappa) + \beta(\kappa)\exp(-2\kappa t)$ . Here, we have chosen the total system size  $L = 1000$ .

amplitude (see Fig. 3(b)). It is important to realise that the finite MI observed in the steady state (see Fig. [1] of the main text) is an artefact of this non-vanishing tail of the correlation profile. Further, the surviving TPCs in the steady state is an exponentially decaying function (see Fig. [3] in the main text) with the intermediate distance  $|n - m|$  between the two points suggesting the existence of a finite correlation length,  $\xi_\kappa = 2/\kappa$ , beyond which the TPCs in the steady state have negligible contributions. We have also checked that the real and imaginary part of the other TPC  $F_{mn}(t)$  given in Eq. (S27) also has the same dynamical behavior as discussed above.

The scaling of the MI in the steady state with the sub-system size  $\ell$  (see Fig. S2) is now explained as follows. In the steady state, only the points inside the sub-system which are located within a distance  $\xi_\kappa$  from the boundary of the sub-system become correlated with the rest of the system. The two relevant length scales in the steady state are therefore  $\xi_\kappa$  and  $\ell$ . If  $\ell \ll \xi_\kappa$ , all the points inside the sub-system, therefore, contribute to the steady state MI; consequently it follows a volume law in this limit. On the other limit, if  $\ell \gg \xi_\kappa$ , only the points located in the vicinity of the boundary of the sub-system contribute to the steady state MI thus leading to an area law ( $\ell$  independent) behavior. In the intermediate case when  $\ell$  is comparable with  $\xi_\kappa$ , the steady state MI shows a sub-volume behaviour.

Finally, we note that the existence of a non-vanishing value of the MI in the steady state despite the quasi-particles having a finite life-time is a striking result in presence of dissipation. We suspect that this happens because the action of the bath is similar to a *continuous* quench on the system which results in generation of quasi-particles at all times. In the steady state, a balance is reached between the generation and destruction processes of the quasi-particles which result in the steady non-vanishing value. Although a rigorous analytical proof of this claim is not feasible, we however, adopt an indirect way to support our claim as follows.

We recall (in the Fig. S3) that as the system evolves, the amplitude of oscillations of TPCs decreases rapidly in the dissipative case unlike the unitary case. To capture this difference in a more compact way, we calculate the following quantity

$$P_m(t) = \sum_{n=m}^{m+t} |\langle c_{m-n}^\dagger(t) c_{m+n}(t) \rangle|^2, \quad (\text{S36})$$

which at a given time can be considered to be a measure of the total number of quasi-particles originated from the point  $m$ . In the Fig. S4, we follow the temporal evolution of  $P_m(t)$  for different values of  $\kappa$ . In the unitary case ( $\kappa = 0$ ), it remains constant with time which indicates that total number of quasi-particles remains constant for all time; this further implies that the quasi-particles originated by the sudden quence of the transverse field have infinite life time. However, in the dissipative case ( $\kappa \neq 0$ ),  $P_m(t)$  shows an exponential decay to a constant non-zero steady state value. This exponential decay can be interpreted as the result of the decay of the quasi-particles generated due to the sudden quench at  $t = 0$ . Therefore, for  $\kappa \neq 0$ , a time scale  $\tau_\kappa = 1/2\kappa$  (other than  $t^*$ ) emerges after which the generation of quasi-particles due to the persistent coupling to the bath and their destruction balances each other, which manifests in the form of a steady value for the MI.

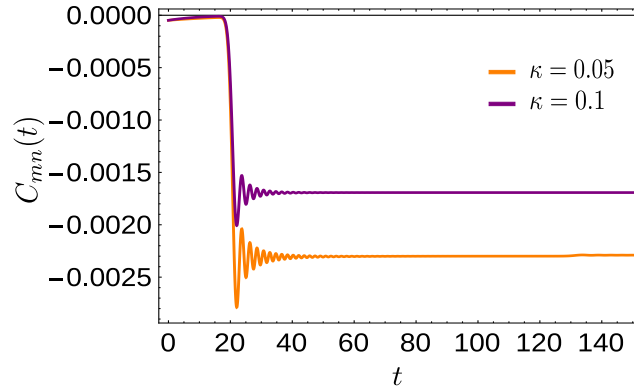


FIG. S5. This figure shows the time evolution of the two point correlation  $C_{mn}(t)$  for different values of  $\kappa$  under no quench situation for different values of  $(m - n)$ . This figure should be compared with Fig. [3] of the main text.

### ROLE OF BATH

To comprehend the role played by the bath, we investigate  $C_{mn}(t)$  with  $m$  and  $n$  fixed as a function of time in the *no-quench* situation. In the no-quench situation, there is no quenching of the transverse field and the Ising chain is initially prepared in the ground state of Hamiltonian  $H_k(h)$  with field  $h = 1$ , which thereafter evolves with the same Hamiltonian. After the decay of the (small) initial correlation of the critical ground state, we once again observe that a finite correlation starts developing for  $t > t^* = \ell/2$  as depicted in Fig. S5. This, in hindsight, suggests that the action of attaching the bath is similar to a global quench that results in the generation of quasi-particles throughout the system.

- 
- [S1] G. Lindblad, *Commun. Math. Phys.* **48**, 199 (1976).
  - [S2] C. W. Gardiner and P. Zoller, *Quantum Noise* (Springer, Heidelberg, 2000).
  - [S3] H. P. Breuer and F. Petruccione, *Theory of open quantum systems*, Oxford University Press, Oxford (2002).
  - [S4] A. Carmele, M. Heyl, C. Kraus, M. Dalmonte, *Phys. Rev. B* **92**, 195107 (2015).
  - [S5] M. Keck, S. Montangero, G. E. Santoro, R. Fazio, D. Rossini, *New J. Phys.* **19** 113029 (2017).
  - [S6] S. Bandyopadhyay, S. Laha, U. Bhattacharya and A. Dutta, *Sci. Rep.* **8**, 11921 (2018).
  - [S7] I. Peschel, *J. Phys. A: Math. Gen.* **36**, L205-L208 (2003).